doi:10.20944/preprints201902.0237.v1

Peer-reviewed version available at *Int. J. Mol. Sci.* **2019**, *20*, 1542; doi:10.3390/ijms20071542

Article

Quantum chemical and kinetic study on radical/molecule formation mechanism of pre-intermediates for PCTA/PT/DT/DFs from 2-chlorothiophenol and 2-chlorophenol precursors

Chenpeng Zuo[1], Hetong Wang[1], Wenxiao Pan[2], Siyuan Zheng[1], Fei Xu[1,3]*, Qingzhu Zhang[1]

[1] Environment Research Institute, Shandong University, Qingdao 266237, P. R. China; zuochenpeng@126.com, Kishi_Wang@163.com, zhengsiyuan1991@126.com, xufei@sdu.edu.cn, zqz@sdu.edu.cn

[2] State Key Laboratory of Environmental Chemistry and Ecotoxicology, Research Center for Eco-Environmental Sciences, Chinese Academy of Sciences, Beijing 100085, P. R. China; wxpan@rcees.ac.cn

[3] Shenzhen Research Institute, Shandong University, Shenzhen 518057, P. R. China

* Correspondence: xufei@sdu.edu.cn; Tel.: +86-532-58631992

Abstract: Polychlorinated phenoxathiins (PCPTs), polychlorinated dibenzothiophenes (PCDTs), and polychlorinated thianthrenes (PCTAs) are sulfur analogues of polychlorinated dibenzo-p-dioxins and polychlorinated dibenzofurans (PCDD/DFs). Chlorothiophenols(CTPs) and chlorophenols (CPs) are key precursors to form PCTA/PT/DTs, which can form chloro(thio)phenoxy radical, sulfydryl/hydryl-substituted phenyl radical and (thio)phenoxyl diradicals. The available radical/radical PCTA/DT formation mechanism failed to explain the higher concentration of PCDTs than that of PCTAs under the pyrolysis or combustion conditions. Thus in this work, a detailed thermodynamics and kinetic calculations were carried out to investigate the pre-intermediates formation for PCTA/PT/DTs from radial/molecule coupling of 2-C(T)P with their key radical species. Our study found that the radial/molecule mechanism can thermodynamically and kinetically contribute to the gas-phase formation of PCTA/PT/DT/s. The S/C coupling modes to form thioether-(thio)enol intermediats are preferable over the O/C coupling modes to form ether-(thio)enol intermediats. Thus, although the radial/molecule coupling of chlorophenoxy radical with 2-C(T)P have no effect on the PCDD/PTs formation, the radial/molecule coupling of chlorothiophenoxy radical with 2-C(T)P play an important role in the PCDT/PT formation. Most importantly, the pre-PCDT intermediates formation pathways from the coupling of sulfydryl/hydryl-substituted phenyl radical with 2-C(T)P and the coupling of (thio)phenoxyl diradicals with 2-C(T)P are more favorable to pre-PCTA/PT intermediates formation pathways from the coupling of chlorothiophenoxy radical with 2-C(T)P, which can give reasonable explanation for the high PCDT-to-PCTA ratio in the environment.

Keywords: PCTA/PT/DTs; Formation mechanism; Radical/molecule coupling; Density functional theory; Rate constant

---

1. Introduction

Polychlorinated thianthrenes/dibenzothiophenes (PCTA/DTs) are polychlorinated dibenzo-p-dioxins/dibenzofurans (PCDD/DFs) analogues with the oxygen atoms substituted by the sulfur atoms, which have given rise to environmental public and regulatory concern. PCTA/DTs are found as mixtures of 75 PCTA and 135 PCDT isomers, which have similar geochemical behavior, toxicity, persistent, lipophilic and physicochemical properties as PCDD/DFs [1–7]. PCTA/DTs have been widely detected in the different environmental samples, such as aquatic organisms [8], soil and sediment [9,10], pulp bleaching [11], wastes from petroleum refineries [12], petroleum spills [13], especially in some high temperature pyrolysis or combustion conditions such as incineration of municipal waste and fly ash [14,15], stack gas [16] and metal reclamation industry [17]. The concentrations of PCDTs in fly ash and in stack gas samplesa are found to be much higher than those observed in some pulp mill effluents [18]. Sinkkone *et al.* reported the concentrations of TCDBTs, TeCDBTs and PeCDBTs in gas phase samples from the aluminium smelter to be in the range of 40~850 ng/nm^3, 9~370 ng/nm^3 and 1~155 ng/nm^3, respectively, and the amount approach the concentration of PCDD/DFs in emissions and wastes [17]. Similar as PCDD/DFs, PCTA/DTs were never intentionally synthesized for commercial purposes, but formed as byproducts from the thermal and combustion conditions. Polychlorinated phenoxathiins (PCPTs) are also one group of chlorinated tricyclic aromatic heterocycles which can be identified as PCDD analogues with one oxygen substituted by sulfur atom or PCTAs with one sulfur substituted by oxygen atom. It is reported that PCPTs have thermodynamic properties, persistence and environmental mobility as PCTA/DTs, which can be viewed as dioxin-like componds [19]. Although corresponding researches pertinent to the formation of PCPTs are not as much as PCDD/DFs and PCTA/DTs, the structural and property resemble of PCPTs with PCDD/DFs and PCTA/DTs reveals their formation possible similarity. For example, PCPTs have been proved to form with PCTAs and PCDTs in combustion experiments [20]. Ferrario *et al.* stated that phenoxathiins can be converted to dibenzofuran by heating with metallic copper at 250 °C [21]. Hence, the information about formation mechanism of PCTA/PT/DTs under combustion and thermal processes are required, which can serve as a basis for minimizing PCTA/PT/DTs emissions and hinder their harm to the human and environment.

A careful examination of the literature shows that two heterogeneous PCTA/DT formaition pathways were proposed: formation reactions from elemental carbon, sulfur and chlorine and sulfur-containing pesticides [22] and formation reactions from chemical precursors [23–27], which is the most direct route to the formation of PCTA/DTs. Among different precursors, chlorothiophenols (CTPs) are demonstrated to be the most important precursors of PCTA/DTs, which is consistent with the widely recognized fact that chlorophenols (CPs) are identified to be predominant precursors of PCDD/DFs [23,24,28]. CTPs are used in large quantities in various chemical industries, such as in manufacturing of dyes, insecticides, printing inks, pharmaceuticals, and polyvinyl chloride [29], while CPs are released from direct application as biocides, leaching from wood products, synthesis during bleaching operations, and emissions from operating facilities [30,31]. Under high-temperature conditions, CTPs can readily form chlorothiophenoxy radical (CTPRs) as well as sulfydryl-substituted phenyl radical and the thiophenoxyl diradical by losing the sulfydryl-H, the H/Cl atom combine to the carbon in the adjacent position of the carbon with -SH group, and both the sulfydryl-H and the *ortho*-substituted H/Cl, respectively, via abstraction reactions by H, OH, Cl, or O(^{3}P) radicals. Although sulfydryl-substituted phenyl radicals and thiophenoxyl diradicals have not yet been detected in combustion and thermal processes, their oxygenated counterparts hydroxyl-substituted phenyl radicals and phenoxyl diradicals have been identified and proposed to be potential precursors from PCDD/DF formation [32–35]. Yu *et al.* and Pan *et al.* has carried out theoretical studies and proved the formation feasibility of sulfydryl-substituted phenyl radicals and thiophenoxyl diradicals from CTPs and that of hydroxyl-substituted phenyl radicals and phenoxyl diradicals from CPs, and proved their energetically favorable contribution to PCTA/DT and PCDD/DF formation, respectively [27,36].

Similar as the formation of PCDD/DFs from CPs precursor, the homogeneous gas-phase formation of PCTA/DTs was proposed that involve radical/radical condensation of CTPRs and radical/molecule recombination of CTPR and CTP [23–25,37–40]. Dar *et al.* have presented that radical/radical coupling are thermodynamically comparable over radical/molecule recombination for the PCTA/DT formation [23,24]. Therefore, following the radical/radical routes, a serious theoretical studies on PCTA/DT formation mechanisms from the coupling of 2-CTPRs, 2,4,5-TCTPRs, 2,4-DCTPRs and 2,4,6-TCPRs were proposed by Dar *et al.* and our group [23–26]. These studies found that the the PCTA formation was much easier than the PCDT formation owning to the fact that the

PCTA formation can occur via one less elementary step than PCDT formaion and the potential barrier of the rate-determining step of PCTA formation is about 10 kcal/mol lower than that the PCDT formation [23–26]. However, this conclusion failed to give reasonable explanation for the much higher concentration of PCDTs than that of PCTAs under the pyrolysis or combustion conditions [16,17]. For instance, the concentration of tetrachlorobenzothiophene (TeCDT) was detected to be approximately 5~40 times greater than that of tetrachlorothianthrene (TeCTA) in stack gas samples from waste incineration samples [16]. Sinkkone *et al.* observed that the mean concentrations of trichlorobenzothiophene (TCDT) (8.944 ng/g) in some ash and slag samples was much higher than that of triachlorothianthrene (TCTA) (0.052 ng/g) [17]. This great discrepancy prompted us turn our attention back to the the radical/molecule mechanism, which has long been overlooked to the PCTA/DT formation and may be contribute to the high PCDT-to-PCTA ratio. Firstly, the radical/molecule mechanism from 2-CTPR with 2-CTP was calculated using B3LYP method by Dar *et al.* [23,24], which ignored the electron correlation and may overestimate the energy values. Secondly, recent research by Pan *et al.* found that the radical/molecule mechanisms from phenyl radicals and phenoxyl diradicals with 2-CP solely lead to the formation of PCDF, which greatly well account for the experimental observation of the high PCDF-to-PCDD ratio from CPs as precursors both in gas-phase and particle mediated conditions [41]. Along the same line of inquiry, the radical/molecule mechanisms from sulfydryl-substituted phenyl and thiophenoxyl diradicals with CTPs were inspired to be further studied and compared with the oxygen substituted reactions. Thirdly, considering the structure and property similarity of PCPTs with PCTA/DDs and the coexistence of CTPs and CPs, it is of significance to study the PCPT formation from cross-consendation from CPs with CTP relative radicals or CTPs with CP relative radicals. High correlation between the PCTA/DTs, PCDD/DFs and PCPTs revealed their similar formation mechanism [14,20,21,42,43]. As far as we know, there is no information available on the radical/molecule mechanisms for the PCTA/DT formation from sulfydryl-substituted phenyl and thiophenoxyl diradicals with CTPs, as well as the radical/molecule mechanisms for the PCPT formation from CP and CTP as precursors.

Therefore, in this study, we present a systematic theoretical study on the initial pathways of PCTA/PT/DT formation from the condensation reactions of 2-CP/2-CTP with chlorinated phenoxy radical 2-chlorophenoxy (CPR1) and chlorinated thiophenoxy radical 2-chlorothiophenoxy (CTPR1), phenyl radicals 2-hydroxylphenyl (PR2) and 2-sulfydrylphenyl (TPR2), chlorinated phenyl radicals 2-hydroxyl-3-chloro-phenyl (CPR2) and 2-sulfydryl-3-chloro-phenyl (CTPR2), phenoxyl diradical (PDR) and thiophenoxyl diradical (TPDR), chlorinated phenoxyl diradical (CPDR) and chlorinated thiophenoxyl diradical (CTPDR) (shown in Figure 1). 2-CTP and 2-CP were selected as model compounds because they are simplest and most representative CTPs and CPs precursors to produce PCTA/PT/DT/DFs. The kinetic data and rate constants were evaluated over a wide temperature range of 600~1200 K and fitted into Arrhenius formulas to improve and optimize PCTA/DT formation mathematic models. This work provides new mechanism for the formation of PCTA/DTs to explain the higher concentration of PCDTs than that of PCTAs in the environment, and explores plausible mechanism for the formation of dioxin-like componds PCPTs. The contribution to PCTA/PT/DT/DF formation from different radical/molecule condensation reactions was sorted and compared with radical/radical mechanism from self-coupling of 2,4-dichlorothiophenoxys (2,4-DCTPRs) in our previous work [26] and the formation of PCDD/DFs from oxygen substituted precursors [41].

2. Results

2.1. Formation of radical species C(T)PR1, C(T)PR2, C(T)PDR, (T)PR2 and (T)PDR from 2-CTP and 2-CP molecules

Peer-reviewed version available at *Int. J. Mol. Sci.* **2019**, *20*, 1542; doi:10.3390/ijms20071542

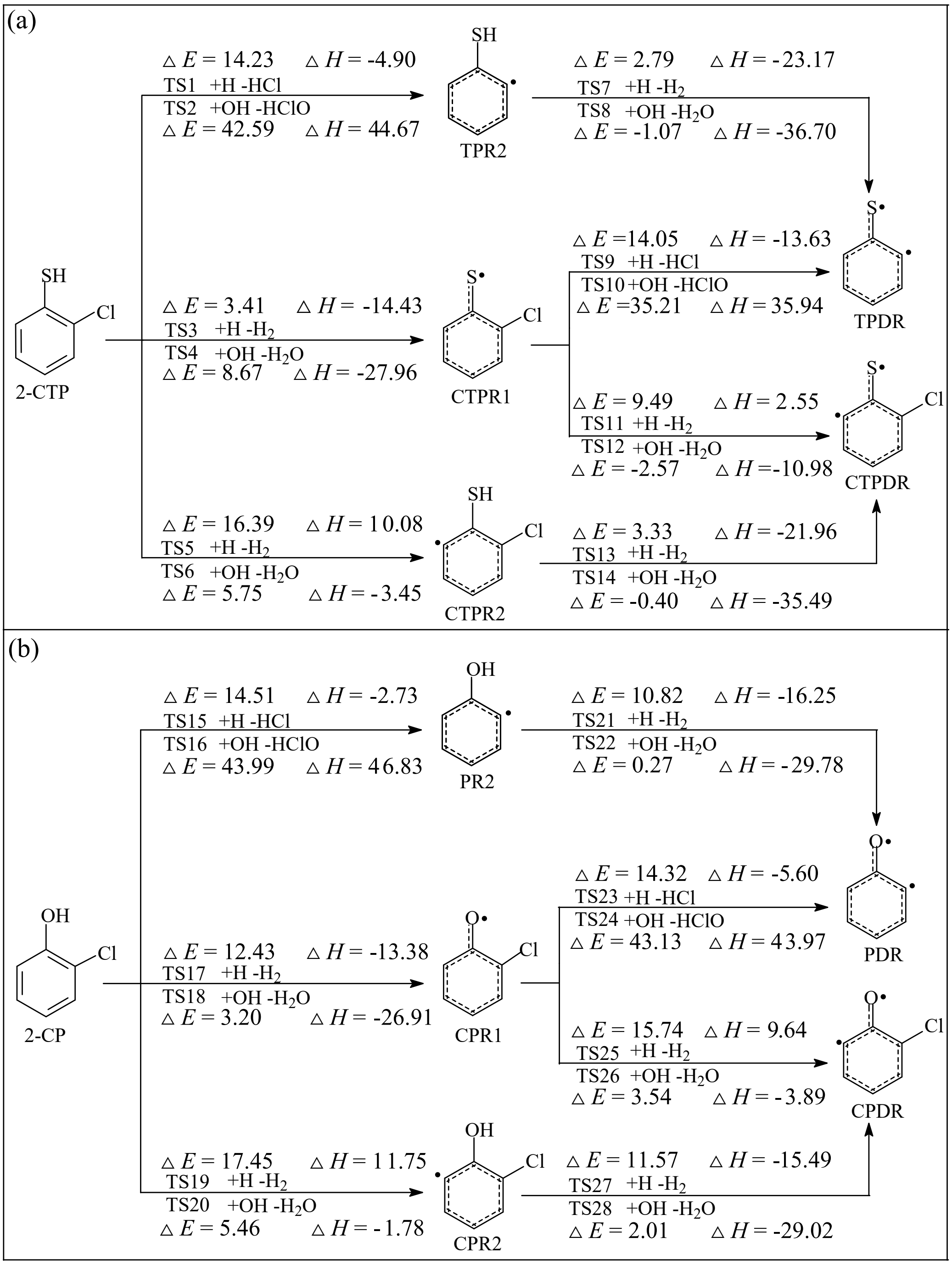

Figure 1. Formation of radical species C(T)PR1, C(T)PR2, C(T)PDR, (T)PR2 and (T)PDR embedded with the potential barriers Δ*E* (in kcal/mol) and reaction heats Δ*H* (in kcal/mol) from reactions of 2-CTP (a) and 2-CP (b) with H/OH radicals, respectively. Δ*H* is calculated at 0 K.

The formation of 2-chlorothiophenoxy (CTPR1), 2-sulfydryl-3-chloro-phenyl (CTPR2), chlorinated thiophenoxyl diradical (CTPDR), 2-sulfydrylphenyl radical (TPR2), thiophenoxyl diradical (TPDR) derived from 2-chlorothiophenol (2-CTP) and the formation of 2-chlorophenoxy (CPR1), 2-hydroxyl-3-chloro-phenyl (CPR2), chlorinated phenoxyl diradical (CPDR), 2-hydroxylphenyl radical (PR2), phenoxyl diradical (PDR) derived from 2-chlorophenol (2-CP) are the initial and key step in the radical/molecule formation of PCTA/PT/DT/DFs. In combustion and thermal processes, these radicals may be generated by means of H or Cl extraction reactions of 2-C(T)P by the active radicals H, OH, Cl or O(^{3}P) which exist abundantly in high temperature conditions. The potential barriers (Δ*E*) and the reaction heat (Δ*H*) which were calculated at the MPWB1K/6-311+G(3df,2p)//MPWB1K/6-31+G(d,p) level operating in the formation of C(T)PR1, C(T)PR2, C(T)PDR, (T)PR2 and (T)PDR from 2-C(T)P abstracted by the H and OH is given in the Figure 1(a) and (b). In Figure 1, data of sulfydryl/hydroxyl-H abstraction of 2-C(T)P by H and OH were cited from our previous studies at the MPWB1K/6-311+G(3df,2p)//MPWB1K/6-31+G(d,p) level [44–46] Pan *et al.* and Yu *et al.* also studied the formation of C(T)PR1, C(T)PR2, C(T)PDR, (T)PR2 and (T)PDR from 2-C(T)P molecules abstracted by H radical at the BB1K/6-311+G(3df,2p)//BB1K/6-311G(d,p) level [27,41]. Similar abstraction reactions by OH radical were added in this study. Notably, Our value at the MPWB1K/6-311+G(3df,2p)//MPWB1K/6-31+G(d,p) level match well with Pan and Yu's data at the BB1K/6-311+G(3df,2p)//BB1K/6-311G(d,p) level, and the maximum relative error remains within 1.03 kcal/mol for potential barriers (ΔE) and less than 0.90 kcal/mol for reaction heats (ΔH). From this results, the same accuracy can be expected for other species involved in this study. As can be seen in Figure 1, the chlorinated phenoxy/thiophenoxy radicals C(T)PR1 arises from cleavage of or sulfydryl S-H bond or hydroxyl O-H bond from the precursor 2-C(T)P. Moreover, the sulfydryl-substituted/hydroxyl-substituted phenyl radicals (T)PR2 and C(T)PR2 derive from dissociation of the Cl or H atom combine to the carton in the adjacent position of the carbon with the sulfydryl/hydroxyl group. Additionally, the phenoxyl/thiophenoxyl diradicals (T)PDR and C(T)PDR are sourced from loss both of the or sulfydryl-H or hydroxyl-H and the *ortho*-substituted Cl or H atom. All the optimized geometries for 2-C(T)P and related radicals are shown in Figure 2.

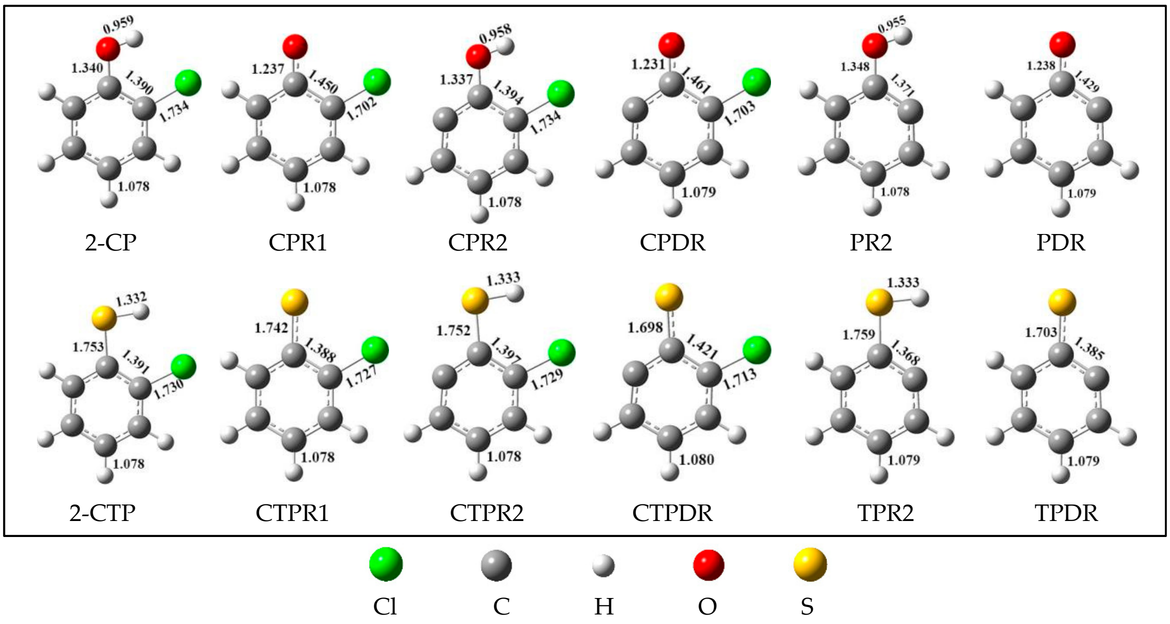

Figure 2. Optimized structures of 2-CP and 2-CTP molecules and related radicals in this paper: 2-chlorophenol (2-CP), 2-chlorophenoxy (CPR1), 2-hydroxyl-3-chloro-phenyl (CPR2), chlorinated phenoxyl diradical (CPDR), 2-hydroxylphenyl radical (PR2), phenoxyl diradical (PDR), 2-chlorothiophenol (2-CTP), 2-chlorothiophenoxy (CTPR1), 2-sulfydryl-3-chloro-phenyl (CTPR2), chlorinated thiophenoxyl diradical (CTPDR), 2-sulfydrylphenyl radical (TPR2), thiophenoxyl diradical (TPDR). All the values are in Å.

2.2. Formation of pre-intermediates of PCTA/PT/DT/DFs via radical/molecule coupling reactions

The radical/radical or radical/molecule recondensation of C(T)P and C(T)PRs plays a crucial role in the the homogeneous gas-phase formation of PCTA/PT/DTs. The radical/molecule coupling reaction routes via cross-condensation of 2-C(T)P molecule with chlorinated (thio)phenoxy radicals C(T)PR1, chlorinated or unchlorinated hydroxyl(sulfydryl)-substituted phenyl radicals C(T)PR2/(T)PR2 and chlorinated or unchlorinated (thio)phenoxyl diradicals C(T)PDR/(T)PDR are exhibited in Figures 3~5, respectively. The potential barrier ΔE (in kcal/mol) and reaction heats ΔH (in kcal/mol) are calculated at the MPWB1K/6-311+G(3df,2p)//MPWB1K/6-31+G(d,p) level in Figures 3~5. In order to comparing with the PCDD/DF formation from 2-CP and corresponding oxygen substituted radicals from Pan's study [41], the radical/molecule coupling reaction routes via cross-condensation of 2-CP with chlorophenoxy radical CPR1, chlorinated or unchlorinated hydroxyl-substituted phenyl radicals CPR2/PR2 and phenoxyl diradicals CPDR/PDR are calculated at MPWB1K/6-311+G(3df,2p)//MPWB1K/6-31+G(d,p) level and presented in Figures S1. Several typical optimized transition state geometries in PCTA/PT/DT/DF formation are shown in Figure S3.

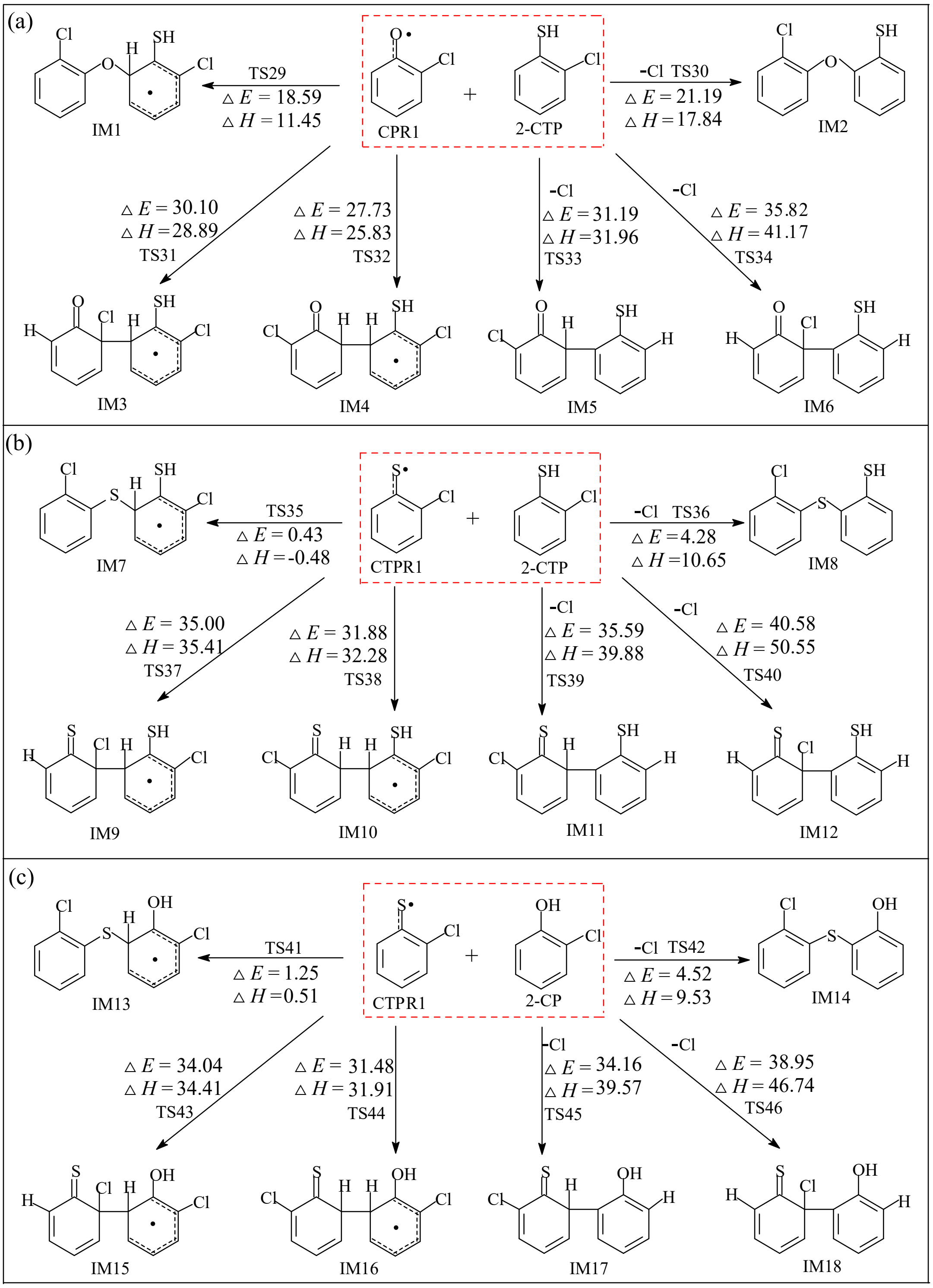

Figure 3. Pre-PCTA/PT/DT/DF formation routes embedded with the potential barriers Δ*E* (in kcal/mol) and reaction heats Δ*H* (in kcal/mol) from the cross-condensation reactions of CPR1 with 2-CTP (a), CTPR1 with 2-CTP (b) and CTPR1 with 2-CP (c). Δ*H* is calculated at 0 K.

2.2.1. Coupling reaction of C(T)PR1 with 2-C(T)P

Peer-reviewed version available at *Int. J. Mol. Sci.* **2019**, *20*, 1542; doi:10.3390/ijms20071542

In Figure 3, the cross-condensation reactions of CPR1 with 2-CTP, CTPR1 with 2-CTP and CTPR1 with 2-CP are depicted in Figure 3(a), Figure 3(b) and Figure 3(c), respectively. There exhibit four kinds of sulfur/oxygen-carbon coupling modes (S/C or O/C for short): (1) the coupling of the phenolic oxygen with the *ortho* carbon bonded to hydrogen of 2-C(T)P molecule (O/σ-CH for short), (2) the coupling of the thiophenolic sulfur with the *ortho* carbon bonded to hydrogen of 2-C(T)P molecule (S/σ-CH for short), (3) the coupling of the phenolic oxygen with the *ortho* carbon bonded to chlorine of 2-C(T)P molecule (O/σ-CCl for short) and (4) the coupling of the thiophenolic sulfur with the *ortho* carbon bonded to chlorine of 2-C(T)P molecule (S/σ-CCl for short). In Figure 3, all the four coupling modes produce four (thio)ether-(thio)enol structures: IM1 are formed from the O/σ-CH coupling, IM2 are produced from O/σ-CCl coupling, IM7 and IM13 are generated from the S/σ-CH coupling, and the IM8 and IM14 are shaped from the S/σ-CCl coupling. The O/σ-CH and S/σ-CH couplings are stepwise reactions, while the O/σ-CCl and S/σ-CCl couplings are one-step synergetic reactions accompanied by the Cl elimination reactions. These intermediates are pre-intermediates for the formation of PCTA/PTs.

There are four kinds of carbon–carbon coupling modes to produce twelve (thio)enol-(thio)keto adducts: (1) the coupling of carbon (hydrogen)-centered radical and carbon (hydrogen)-centered molecule (C_RH/C_MH for short), (2) the coupling of carbon (chlorine)-centered radical and carbon (hydrogen)-centered molecule (C_RCl/C_MH for short), (3) the coupling of carbon (hydrogen)-centered radical and carbon (chlorine)-centered molecule (C_RH/C_MCl for short), and (4) the coupling of carbon (chlorine)-centered radical and carbon (chlorine)-centered molecule (C_RCl/C_MCl for short). In Figure 3, the IM4, IM10 and IM16 are generated from C_RH/C_MH coupling, The IM3, IM9 and IM15 are formed from C_RCl/C_MH coupling, the IM5, IM11 and IM17 are generated from the C_RH/C_MCl coupling, and the IM6, IM12 and IM18 are built from the C_RCl/C_MCl coupling. The C_RH/C_MCl and CCl_R/CCl_M couplings are also accompanied by a synchronously elimination of Cl atom. These intermediates serve as building foundation for analogues of PCDT/DF structures.

2.2.2. Coupling reactions of C(T)PR2 and (T)PR2 with 2-C(T)P

The pre-PCDT/DF formation reaction pathways for cross-couplings between CPR2 and 2-CTP, between CTPR2 and 2-CTP, between CTPR2 and 2-CP, between PR2 and 2-CTP, between TPR2 and 2-CTP, and between TPR2 and 2-CP embedded with the potential barriers ΔE (in kcal/mol) and reaction heats ΔH (in kcal/mol) are illustrated in Figure 4(a)~(f), respectively. After the *ortho*-H/Cl abstraction in benzene ring of 2-CP and 2-CTP, there exits the extremely high reactivity carbon (radcial)-centered hydroxyl(sulfydryl)-substituted phenyl radicals[47,48], C(T)PR2 and (T)PR2, which may attack the 2-C(T)P molecule by two C-C coupling modes to (thio)keto-(thio)enol intermediates: (1) the coupling of carbon (radical)-centered radical and carbon (hydrogen)-centered molecule (C•/CH for short), and (2) the coupling of carbon (radical)-centered radical and carbon (chlorine)-centered molecule (C•/CCl for short). The C•/CCl coupling is synergetic reactions with the Cl elimination occurring at the same time. Six intermediates (IM19, IM21, IM23, IM25, IM27 and IM29) are afforded by C•/CH coupling, and five other intermediates (IM20, IM22, IM24, IM26 and IM28) are produced by C•/CCl coupling. All the eleven intermediates can result in the formation of PCDT/DFs, which are not the precursors for PCTA/PTs owning to the absence of O/S centered radicals in C(T)PR2 and (T)PR2.

2.2.3. Coupling reactions of C(T)PDR and (T)PDR with 2-C(T)P

In this section, the condensation reaction pathways between CPDR and 2-CTP, between CTPDR and 2-CTP, between CTPDR and 2-CP, between PDR and 2-CTP, between TPDR and 2-CTP and between TPDR and 2-CP are discussed and the corresponding results are respectively illustrated in Figure 5(a)~(f). C(T)PDR and (T)PDR are diradicals with two typical radical sites located at the (thio)phenoxyl O or S atom and the *ortho* (thio)phenyl C atom. In Figure 5(a) and (d). The O-C coupling is comprised of two modes (O/σ-CH and O/σ-CCl) to form ether-thioenol adducts and two kinds of C-C coupling modes(C•/CH and C•/CCl) to form dihydroxybiphenyl molecules. In Figure 5(b), (c), (e) and (f), there are two kinds of S-C coupling modes (S/σ-CH and S/σ-CCl) to form ether-

Peer-reviewed version available at Int. J. Mol. Sci. 2019, 20, 1542; doi:10.3390/ijms20071542

thioenol adducts and two kinds of carbon-carbon coupling modes(C•/CH and C•/CCl) to form keto-thioenol molecules. The O/σ-CCl, S/σ-CCl and C•/CCl couplings are synergetic reactions accompanied by the Cl elimination occurring at the same time. The O/C or S/C condensations are endothermic reactions, and the C/C coupling are exothermic. As can be seen in Figure 5, the O/C coupling pathways affords four species IM32, IM33, IM44 and IM45, and the S/C coupling produces eight intermediates IM36, IM37, IM40, IM41, IM48, IM49, IM52 and IM53, which would be followed by the abstraction of H, ring closure and SH/OH elimination of to form PCDT/DFs. The C/C coupling pathways affords four species IM30, IM31, IM34, IM35, IM38, IM39, IM42, IM43, IM46, IM47, IM50 and IM51 which would be followed by the abstraction of H, ring closure and intramolecular elimination of SH/OH elimination to form PCDT/DFs.

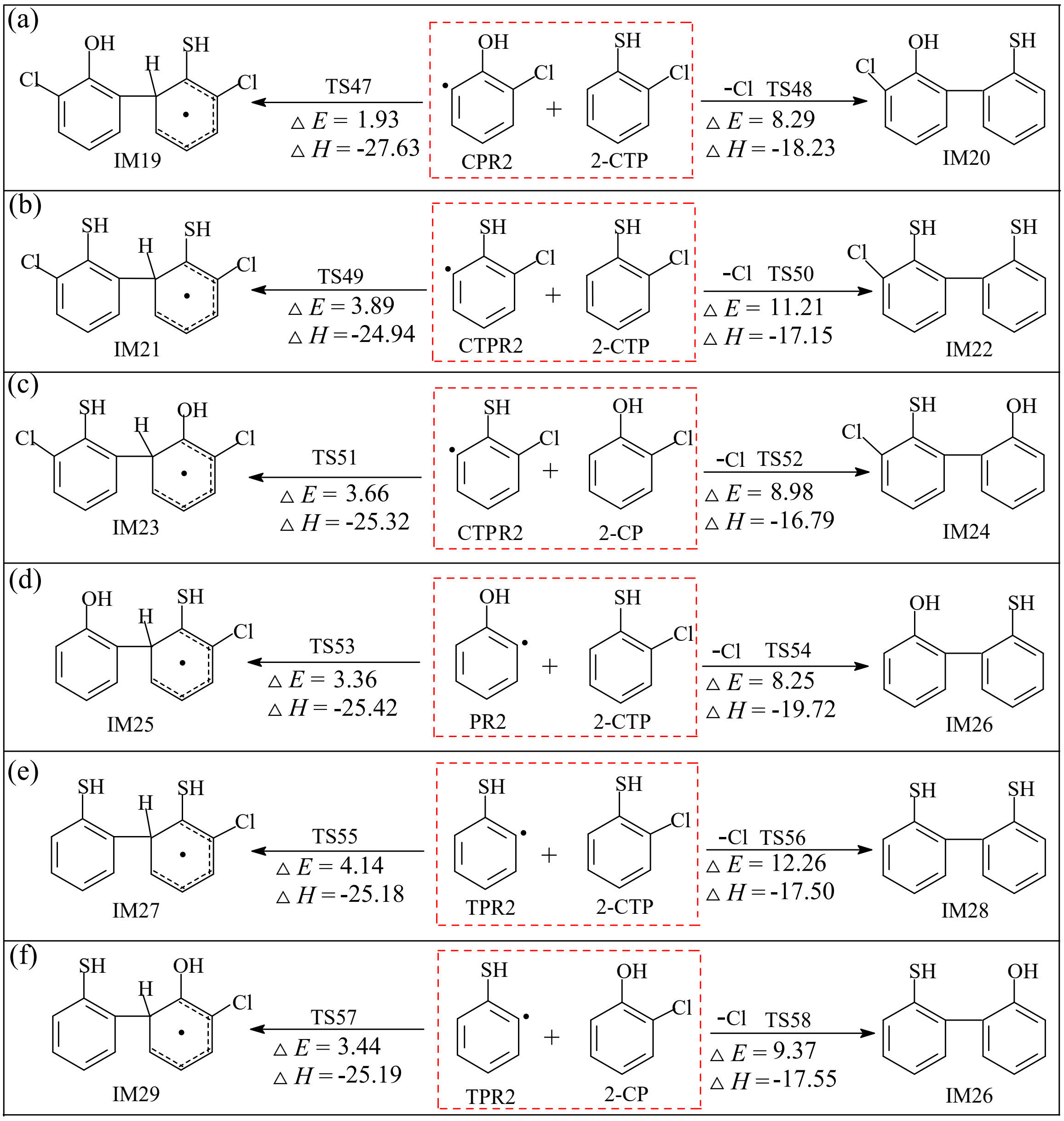

Figure 4. Pre-PCDT/DF formation routes embedded with the potential barriers ΔE (in kcal/mol) and reaction heats ΔH (in kcal/mol) from the coupled reactions of CPR2 with 2-CTP (a), CTPR2 with 2-CTP (b) and CTPR2 with 2-CP (c), PR2 with 2-CTP (d), TPR2 with 2-CTP (e) and TPR2 and 2-CP (f). ΔH is calculated at 0 K.

Peer-reviewed version available at *Int. J. Mol. Sci.* **2019**, *20*, 1542; doi:10.3390/ijms20071542

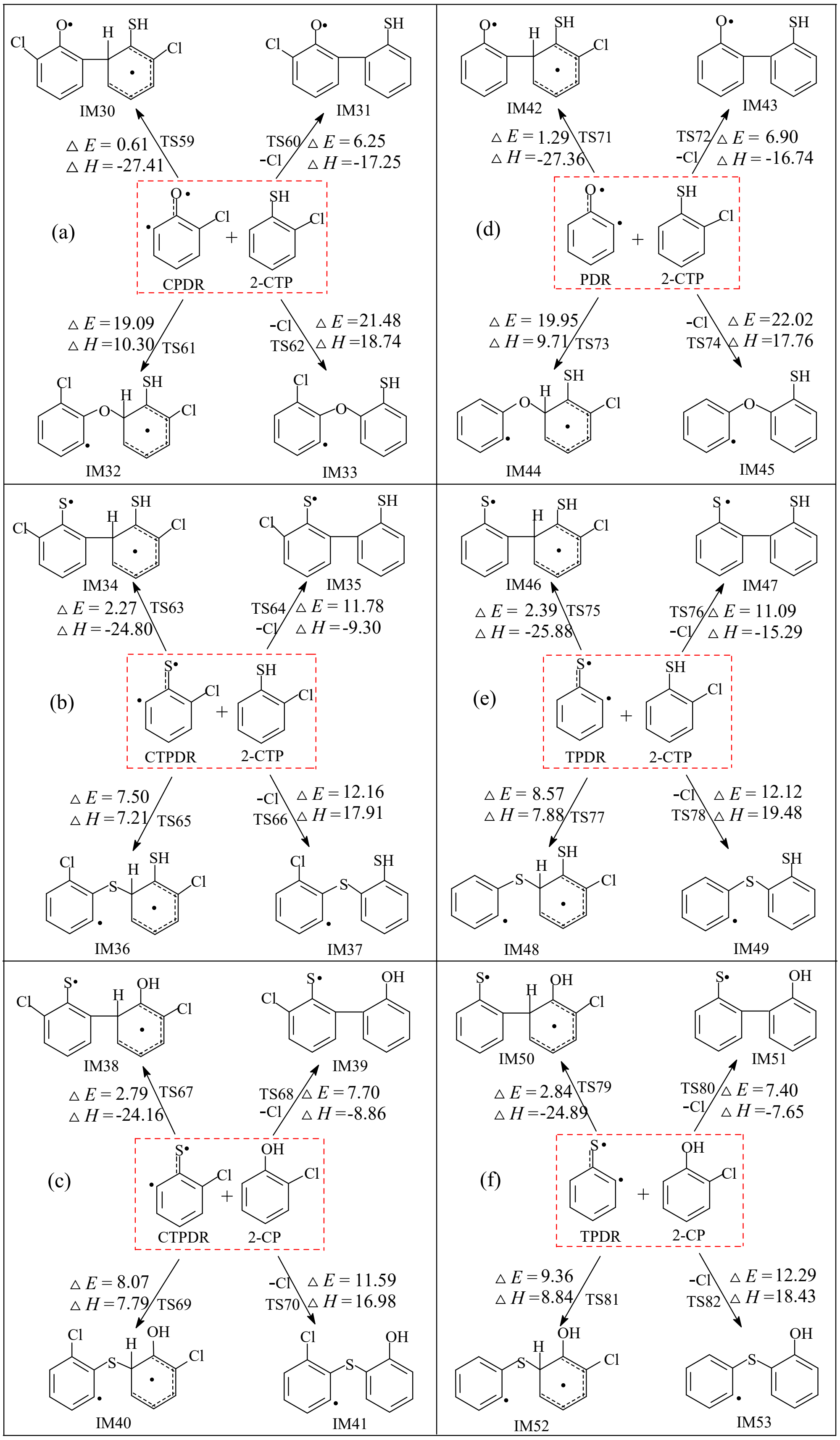

Figure 5. Pre-PCDT/DF formation routes embedded with the potential barriers Δ*E* (in kcal/mol) and reaction heats Δ*H* (in kcal/mol) from the coupled reactions of CPDR with 2-CTP (a), CTPDR with 2-CTP (b) and CTPDR with 2-CP (c), PDR with 2-CTP (d), TPDR with 2-CTP (e) and TPDR and 2-CP (f). Δ*H* is calculated at 0 K.

Peer-reviewed version available at *Int. J. Mol. Sci.* **2019**, *20*, 1542; doi:10.3390/ijms20071542

2.3. Rate constant calculations

The kinetic parameters of pre-PCTA/PT/DT/DF formation routes is significant to construct the formation kinetic model to predict the potential emission and harm to the environment. The rate constants of the formation of the pre-PCTA/PT/DT/DF intermediates from cross-condensation reactions of 2-C(T)P molecules with related radicals were calculated by using conventional transition state theory (TST) method with one-dimensional Wigner's formalism contribution in the temperature range of 600~1200 K [49,50]. The calculated rate constants every 100 K are shown in Table S2 of Supplementary Materials from 600~1200 K.

To be used more effectively, the rate constants were fitted, and Arrhenius formulas are given in Table 1 for the pre-PCTA/PT/DT/DF intermediates formation routes from cross-condensation of 2-C(T)P with C(T)PR1, C(T)PR2 and (T)PR2 radicals and Table 2 for the pre-PCDT/DF intermediates formation routes from cross-couplings of 2-C(T)P with C(T)PDR and (T)PDR radicals. The pre-exponential factor, the activation energy and the rate constants can be obtained from these Arrhenius formulas. The average rate constant (1000 K) for the three coupling modes, i.e., for the O/C type, S/C type and C/C type coupling reactions are listed in Tables 3.

Table 1. Arrhenius formulas for pre-PCTA/PT/DT/DF formation routes from the cross-condensation reactions of 2-C(T)P with C(T)PR1, C(T)PR2 and (T)PR2 over the temperature range of 600~1200 K. (unit is cm^3 $molecule^{-1}$ s^{-1})

Reactions Arrhenius Formulas	Arrhenius Formulas
CPR1 + 2-CTP → IM1 via TS29	$k(T) = (2.09 \times 10^{-15}) \exp(-11163/T)$
CPR1 + 2-CTP → IM2 + Cl via TS30	$k(T) = (1.79 \times 10^{-15}) \exp(-12526/T)$
CPR1 + 2-CTP → IM3 via TS31	$k(T) = (1.43 \times 10^{-15}) \exp(-17118/T)$
CPR1 + 2-CTP → IM4 + Cl via TS32	$k(T) = (3.90 \times 10^{-15}) \exp(-15840/T)$
CPR1 + 2-CTP → IM5 via TS33	$k(T) = (1.42 \times 10^{-15}) \exp(-17613/T)$
CPR1 + 2-CTP → IM6 + Cl TS34	$k(T) = (1.21 \times 10^{-16}) \exp(-19231/T)$
CTPR1 + 2-CTP → IM7 via TS35	$k(T) = (2.37 \times 10^{-15}) \exp(-2233/T)$
CTPR1 + 2-CTP → IM8 via TS36	$k(T) = (1.22 \times 10^{-15}) \exp(-4093/T)$
CTPR1 + 2-CTP → IM9 via TS37	$k(T) = (1.40 \times 10^{-15}) \exp(-19723/T)$
CTPR1 + 2-CTP → IM10 via TS38	$k(T) = (5.33 \times 10^{-15}) \exp(-18080/T)$
CTPR1 + 2-CTP → IM11 via TS39	$k(T) = (1.99 \times 10^{-15}) \exp(-19993/T)$
CTPR1 + 2-CTP → IM12 + Cl TS40	$k(T) = (5.24 \times 10^{-16}) \exp(-22527/T)$
CTPR1 + 2-CP → IM13 via TS41	$k(T) = (1.14 \times 10^{-14}) \exp(-2790/T)$
CTPR1 + 2-CP → IM14 + Cl via TS42	$k(T) = (1.01 \times 10^{-14}) \exp(-4524/T)$
CTPR1 + 2-CP → IM15 via TS43	$k(T) = (6.13 \times 10^{-15}) \exp(-19327/T)$
CTPR1 + 2-CP → IM16 + Cl via TS44	$k(T) = (1.06 \times 10^{-14}) \exp(-17908/T)$
CTPR1 + 2-CP → IM17 via TS45	$k(T) = (4.46 \times 10^{-15}) \exp(-19296/T)$
CTPR1 + 2-CP → IM18 + Cl TS46	$k(T) = (1.29 \times 10^{-15}) \exp(-21760/T)$
CPR2 + 2-CTP → IM19 via TS47	$k(T) = (1.42 \times 10^{-14}) \exp(-3082/T)$
CPR2 + 2-CTP → IM20 + Cl via TS48	$k(T) = (3.37 \times 10^{-15}) \exp(-6141/T)$
CTPR2 + 2-CTP → IM21 via TS49	$k(T) = (7.46 \times 10^{-15}) \exp(-3994/T)$
CTPR2 + 2-CTP → IM22 + Cl via TS50	$k(T) = (1.20 \times 10^{-15}) \exp(-7520/T)$
CTPR2 + 2-CP → IM23 via TS51	$k(T) = (3.19 \times 10^{-14}) \exp(-4022/T)$
CTPR2 + 2-CP → IM24 + Cl TS52	$k(T) = (5.48 \times 10^{-15}) \exp(-6518/T)$
PR2 + 2-CTP → IM25 via TS53	$k(T) = (1.26 \times 10^{-14}) \exp(-3668/T)$
PR2 + 2-CTP → IM26 + Cl via TS54	$k(T) = (1.53 \times 10^{-15}) \exp(-5987/T)$
TPR2 + 2-CTP → IM27 via TS55	$k(T) = (1.21 \times 10^{-14}) \exp(-4148/T)$
TPR2 + 2-CTP → IM28 + Cl via TS56	$k(T) = (1.21 \times 10^{-15}) \exp(-7993/T)$
TPR2 + 2-CP → IM29 via TS57	$k(T) = (4.85 \times 10^{-14}) \exp(-3879/T)$
TPR2 + 2-CP → IM26 + Cl via TS58	$k(T) = (9.06 \times 10^{-15}) \exp(-6757/T)$

Table 2. Arrhenius formulas for pre-PCTA/PT/DT/DF formation routes from the cross-condensation reactions of 2-C(T)P with C(T)PDR and (T)PDR over the temperature range of 600~1200 K. (unit is cm^3 $molecule^{-1}$ s^{-1})

Reactions Arrhenius Formulas	Arrhenius Formulas
CPDR + 2-CTP → IM30 via TS59	$k(T) = (3.33 \times 10^{-14}) \exp(-2430/T)$
CPDR + 2-CTP → IM31 + Cl via TS60	$k(T) = (8.91 \times 10^{-15}) \exp(-5222/T)$
CPDR + 2-CTP → IM32 via TS61	$k(T) = (2.36 \times 10^{-15}) \exp(-11424/T)$
CPDR + 2-CTP → IM33 + Cl via TS62	$k(T) = (5.26 \times 10^{-15}) \exp(-12811/T)$
CTPDR + 2-CTP → IM34 via TS63	$k(T) = (1.05 \times 10^{-14}) \exp(-3225/T)$
CTPDR + 2-CTP → IM35 + Cl via TS64	$k(T) = (2.45 \times 10^{-15}) \exp(-7902/T)$
CTPDR + 2-CTP → IM36 via TS65	$k(T) = (5.65 \times 10^{-15}) \exp(-5904/T)$
CTPDR + 2-CTP → IM37 + Cl via TS66	$k(T) = (2.03 \times 10^{-15}) \exp(-8446/T)$
CTPDR + 2-CP → IM38 via TS67	$k(T) = (1.43 \times 10^{-13}) \exp(-3672/T)$
CTPDR + 2-CP → IM39 + Cl via TS68	$k(T) = (1.72 \times 10^{-14}) \exp(-6042/T)$
CTPDR + 2-CP → IM40 via TS69	$k(T) = (1.31 \times 10^{-14}) \exp(-6256/T)$
CTPDR + 2-CP → IM41 + Cl TS70	$k(T) = (1.04 \times 10^{-14}) \exp(-8632/T)$
PDR + 2-CTP → IM42 via TS71	$k(T) = (3.51 \times 10^{-14}) \exp(-2775/T)$
PDR + 2-CTP → IM43 + Cl via TS72	$k(T) = (4.24 \times 10^{-15}) \exp(-5424/T)$
PDR + 2-CTP → IM44 via TS73	$k(T) = (6.46 \times 10^{-15}) \exp(-11909/T)$
PDR + 2-CTP → IM45 + Cl TS74	$k(T) = (2.54 \times 10^{-14}) \exp(-13132/T)$
TPDR + 2-CTP → IM46 via TS75	$k(T) = (1.37 \times 10^{-14}) \exp(-3265/T)$
TPDR + 2-CTP → IM47 + Cl via TS76	$k(T) = (1.88 \times 10^{-15}) \exp(-7484/T)$
TPDR + 2-CTP → IM48 via TS77	$k(T) = (4.21 \times 10^{-14}) \exp(-6501/T)$
TPDR + 2-CTP → IM49 + Cl TS78	$k(T) = (7.95 \times 10^{-15}) \exp(-8890/T)$
TPDR + 2-CP → IM50 via TS79	$k(T) = (8.93 \times 10^{-14}) \exp(-3646/T)$
TPDR + 2-CP → IM51 + Cl via TS80	$k(T) = (9.45 \times 10^{-15}) \exp(-5768/T)$
TPDR + 2-CP → IM52 via TS81	$k(T) = (2.02 \times 10^{-14}) \exp(-6885/T)$
TPDR + 2-CP → IM53 + Cl TS82	$k(T) = (3.08 \times 10^{-14}) \exp(-9091/T)$

Table 3. Average rate constants calculated at 1000 K for pre-PCTA/PT/DT/DF formation routes from the cross-condensation reactions between C(T)PR1 with 2-C(T)P, between C(T)PR2 and (T)PR2 with 2-C(T)P, and between C(T)PDR and (T)PDR with 2-C(T)P. (unit is cm^3 $molecule^{-1}$ s^{-1})

C(T)PR1 with 2-C(T)P			C(T)PR2 and (T)PR2 with 2-C(T)P	C(T)PDR and (T)PDR with 2-C(T)P		
C/C type	O/C type	S/C type	C/C type	C/C type	O/C type	S/C type
7.28×10^{-23}	1.75×10^{-20}	2.60×10^{-16}	2.34×10^{-16}	9.82×10^{-16}	3.24×10^{-20}	1.59×10^{-17}

3. Discussion

3.1. Formation of radical species C(T)PR1, C(T)PR2, C(T)PDR, (T)PR2 and (T)PDR from 2-CTP and 2-CP molecules

From Figure 1, the potential barrier and reaction heat for the formation of TPR2 are rather comparable with those for the formation of PR2 abstracted by both H and OH radicals. Analogically, the potential barrier and reaction heat for the formation of CTPR2 are is quite comparable to those for the formation of CPR2. However, for the formation of CTPR1 and CPR1, the potential barrier for the formation of CTPR1 abstracted by H (3.41 kcal/mol) is much lower than that for the formation of CPR1 abstracted by H (12.43 kcal/mol), while the the potential barrier for the formation of CTPR1 abstracted by OH (8.67 kcal/mol) is much higher than that for the formation of CPR1 abstracted by OH (3.20 kcal/mol). This indicates that the sulfydryl-substitution or hydroxyl-substitution of phenyl have no influence on the phenyl-H or phenyl-Cl abstracion, but greatly affect the sulfydryl-H and hydroxyl-H abstraction by H and OH. Moreover, the formation for CTPR1 abstracted by H and OH requires lower potential barriers and much more exothermic than the formation for TPR2 and CTPR2 abstracted by H and OH, which means that thiophenoxy radical CTPR1 radical is more labile to form and more stable than the sulfydryl-substituted phenyl radicals TPR2 and CTPR2. Similarly, the formation of phenoxy radical CPR1 is energetically preferred to the formation of phenyl radicals PR2 and CPR2.

CTPDR/TPDR can be formed from both CTPR1 and CTPR2/TPR2. Obviously, the potential barriers of CTPDR/TPDR formation from CTPR2/TPR2 abstracted by H and OH radicals are much lower than that those of CTPDR/TPDR formation from CTPR1. In addition, the reactions of CTPDR/TPDR formation from CTPR2/TPR2 release more energy than that those of CTPDR/TPDR formation from CTPR1. For example, the CTPDR formation from CTPR2 abstracted by H has much lower potential barrier and more exothermic (ΔE 3.33 kcal/mol, ΔH –21.96 kcal/mol) than that of CTPDR formation from CTPR1 abstracted by H (ΔE 9.49 kcal/mol, ΔH 2.55 kcal/mol). This imply that CTPDR/TPDR is more likely to form through CTPR2/TPR2 than through CTPR1 abstracted by H and OH radicals. Similarly, CPDR/PDR is more readily to produce through CPR2/PR2 than through CPR1. For example, the CPDR formation from CPR2 abstracted by OH has much lower potential barrier and more exothermic (ΔE 2.01 kcal/mol, ΔH –29.02 kcal/mol) than that of CPDR formation from CPR1 abstracted by OH (ΔE 3.54 kcal/mol, ΔH –3.89 kcal/mol). Comparing the CTPDR formation from CTPR1 and CTPR2 with CPDR formation from CPR1 and CPR2 shows that CTPDR formation can take place by requiring lower potential barriers and releasing more heats than the corresponding CPDR formation reactions, which demonstrates that CTPDR formation reactions are more labile than CPDR formation reactions.

It should be noted in Figure 1 that the potential barriers operating in the formation of C(T)PR1, C(T)PR2, C(T)PDR, (T)PR2 and (T)PDR fall within –2.57~43.99 kcal/mol, which could be overcome under high temperature conditions. The initial radicals C(T)PR1, C(T)PR2, C(T)PDR, (T)PR2 and (T)PDR can be easily formed under the pyrolysis or combustion conditions. The result obtained in this respect suggests that these radical species may be generated in the same temperature condition and it is of great possibility to create effective collisions between the radicals and molecules.

3.2. Formation of pre-intermediates of PCTA/PT/DT/DFs via radical/molecule coupling reactions

3.2.1. Coupling reaction of C(T)PR1 with 2-C(T)P

As presented in Figure 3, for the O(S)/C couplings, the O/σ-CH coupling is enthalpically more comparable than O/σ-CCl, and S/σ-CH couplings is favored over S/σ-CCl coupling. For instance, the potential barrier of S/σ-CH and S/σ-CCl couplings of CTPR1 with 2-CTP in Figure 3(b) is 0.43 and 4.28 kcal/mol, respectively; the reaction heat of S/σ-CH and S/σ-CCl couplings of CTPR1 with 2-CTP in Figure 3(b) is –0.48 and 10.65 kcal/mol. Furthermore, the ranking of the four carbon–carbon coupling modes is as follows: CRH/CMH > CRCl/CMH > CRH/CMCl > CRCl/CMCl. For example, the potential barriers for the formation of IM10 from CRH/CMH, the formation of IM9 from CRCl/CMH, the formation of IM11 from CRH/CMCl and the formation of IM12 from CCl/CCl in Figure 3(b) is 31.88, 35.00, 35.59, and 40.58 kcal/mol, respectively; their reaction heats is 32.28, 35.41, 39.88 and 50.55 kcal/mol, respectively.

In Figure 3(a), the potential barriers involved in O/C coupling modes to form ether-thioenol type intermediates process amounting to 18.59~21.19 kcal/mol, which are generally lower than those operating in the C/C coupling modes (27.73~35.82 kcal/mol) to form biphenyl intermediates. In addition, the O/C coupling modes (11.45~17.84 kcal/mol) are less endoergic than the C-C coupling modes (25.8~41.17 kcal/mol). Therefore, the O/C coupling modes to form pre-PCPT intermediates are energetically preferable over the C/C coupling modes to form pre-PCDF intermediates in Figure 3(a). Similar conclusion could be obtained in the CPR1+2-CP reactions in Figure S1(a) of Supplementary

Materials [41]. Analogously, the S/C coupling modes to produce pre-PCTA/PT intermediates energetically preferred to the C/C coupling modes in Figure 3(b) and 3(c) to form pre-PCDT intermediates. In other words, the radical/molecule coupling of C(T)PR1 with 2-C(T)P is difficult to occur in the C/C coupling. The combination reactions of C(T)PR1 with 2-C(T)P tend to take place via the phenoxy oxygen or thiophenoxy sulfur sites and to produce (thio)ether-(thio)enol type intermediates analogues, which process via elimination of H, (thio)phenolic H abstraction, ring close and Cl elimination steps and eventually lead to the formation of PCTA/PTs [41]. To sum up, the ranking of the S/C or O/S coupling to form pre-PCTA/PT/DDs intermediates is as follows: CTPR1+2-CTP > CTPR1+2-CP >> CPR1+2-CP ≈ CPR1+2-CTP.

In particular, the S/C coupling require overcoming dramatically lower potential barriers (0.43~4.28 kcal/mol in Figure 3(b) and 1.25~4.52 kcal/mol in Figure 3(c)) than O/C coupling (18.59~21.19 kcal/mol in Figure 3(a) and 19.53~20.87 kcal/mol in Figure S1(a)) by approximate 20 kcal/mol. In addition, the S/C coupling are less endoergic (–0.48~10.65 kcal/mol in Figure 3(b) and 0.51~9.53 kcal/mol in Figure 3(c)) than the O/C coupling (11.45~17.84 kcal/mol in Figure 3(a) and 13.18~19.10 kcal/mol in Figure S1(a)). Thus, the S/C coupling modes are overwhelmingly superior to the O/C coupling, which indicates that the formation of thioether-enol type intermediates is much easier than that of ether-thioenol type intermediates. In other words, the thiophenolic sulfur centered radcial/molecule coupling is more labile to happen than the phenolic oxygen centered radcial/molecule coupling. Based on this results, we could deduce that although the radical/molecule coupling is uncompetitive comparing with the radial/radical coupling for PCDD formation from CPs by the literature opinions [41], the radical/molecule coupling can play an important role in the PCTA/PT formation from CTPs and CPs. Specially, the radcial/molecule coupling formation of PCPTs can be only achieved via the route of sulfur-centred thiophenoxy radicial attack to 2-CP, but not the route of oxygen-centred phenoxy radical attack to 2-CTP.

The coupling reaction of CTPR1 with 2-CTP were also studied by Dar *et al*. at the B3LYP/6-311+G(d,p) level [23,24]. Two obvious differences were observed: (1) The S/σ-CCl couplings of CTPR1 with 2-CTP requires crossing a potential barrier of 15.6 kcal/mol in the study of Dar *et al*. [23,24], whereas the potential barrier 4.28 kcal/mol in our study; (2) Another coupling mode reported by Dar *et al*. is different from the S/σ-CH coupling mode in our study. The coupling mode provided by Dar *et al*. was accompanied by the elimination of HCl with a greatly high potential barrier 26.4 kcal/mol, whereas the S/σ-CH couplings occur with no atom loss and with a trivial potential barrier (0.43 kcal/mol). The S/σ-CH couplings reported in our study are energetically more favorable than the coupling mode reported by Dar *et al*. [23,24]. The discrepance for S/σ-CCl couplings may arise from the different calculation levels. The energies of Dar *et al*. are calculated at the B3LYP level [23,24], while our energy calculations are carried out at the MPWB1K level. It is well known that B3LYP method do not consider the electronic correlation and systematically overestimates or underestimates barrier heights. In order to further compare with the S/σ-CCl coupling mode proposed by Dar *et al*. [23,24], we checked the transition state structures of S/σ-CCl coupling. Figure S2 in supplementary materials shows configurations of transition states from the S/C coupling of CTPR1 with 2-CTP located by Dar *et al*. and us [24]. The -SH in TS-6 reported by Dar *et al*. point to the direction far away from Cl atom, whereas -SH in TS36 in our study point to Cl atom and form an intramolecular H bond, which could stable the structure and reduce the potential barrier [24]. Thus, the energy value of S/σ-CCl coupling in our study may be more accurate than that from Dar *et al*. The potential barriers of S/C coupling in our study (0.43 and 4.28 kcal/mol) are greatly lower than those from Dar *et al*. (26.4 and 15.6 kcal/mol). The almost barrierless energy value in our study indicate that the radical/molecular coupling of CTPR with CP are nearly comparable with the corrspongding steps involved in the radical/radical reactions of CTPRs [26], and can contribute to the PCTA formation, which has been ignored by Dar *et al*. [23,24].

3.2.2. Coupling reactions of C(T)PR2 and (T)PR2 with 2-C(T)P

The coupling reactions of C(T)PR2 with 2-C(T)P or (T)PR2 with 2-C(T)P can only occur the C-C coupling, resulting in the the formation of (thio)keto-(thio)enol intermediates and transferring into

Peer-reviewed version available at Int. J. Mol. Sci. 2019, 20, 1542; doi:10.3390/ijms20071542

PCDT/DFs. It is evident from Figure 4 that the C•/CH coupling can take place much easier than the C•/CCl coupling. For example, all C•/CH coupling show in Figure 4 can occur encountering potential barriers range from 1.93 to 4.14 kcal/mol, which are much lower than those of C•/CCl coupling (8.25~12.26 kcal/mol). In addition, the C•/CH coupling are estimated to release heats by –27.63~–24.94 kcal/mol, which are much more exothermic than C•/CCl coupling by –19.72~–16.79 kcal/mol. It is also interesting to compare the formation potential of four kinds of C(T)PR2 with 2-C(T)P couplings and four kinds of (T)PR2 with 2-C(T)P couplings. According to Figure 4 and Figure S1(b) and (d), the formation potential ranking of C(T)PR2 with 2-C(T)P couplings is CPR2 + 2-CTP > CPR2 + 2-CP > CTPR2 + 2-CP > CTPR2 + 2-CTP; the formation potential ranking of (T)PR2 with 2-C(T)P couplings is PR2 + 2-CP > PR2 + 2-CTP > TPR2 + 2-CP > TPR2 + 2-CTP. All the potential barriers of C•/CH coupling in Figure 4 are so trivial that they could be easily overcome in high temperature conditions, which means that the radical/molecule coupling of C(T)PR2 and (T)PR2 with 2-C(T)P can compete with the radical/radical combination reactions. Additionally, the similar thermodynamic values for the pre-PCDT formation from CTPR2/TPR2 with 2-CTP and pre-PCDF formation from CPR2/PR2 with 2-CP in Figure S1 imply the oxygen or sulfur substitution make consistent effect on the PCDT/DF formation. All the results provide the facts that the sulfydryl/hydroxyl-substituted phenyl radicals can initial the feasible reactions to form pre-PCDT/DF intermediates, following by the elemination of H, phenolic H abstraction, ring close and elimintion of OH/SH to produce PCDT/DFs.

3.2.3. Coupling reactions of C(T)PDR and (T)PDR with 2-C(T)P

Similar as the O(S)/C couplings from C(T)PR1 with 2-C(T)P in Figure 3, the O(S)/σ-CH couplings is enthalpically preferred to O(S)/σ-CCl. For example, in Figure 5(b), the S/σ-CH coupling from CTPDR + 2-CTP coupling (Δ*E* 7.50 kcal/mol, Δ*H* 7.21 kcal/mol) can occur encountering much lower potential barrier and is less endothermic than O/σ-CH coupling (Δ*E* 12.16 kcal/mol, Δ*H* 17.91 kcal/mol), which means the S/σ-CH coupling are more feasible than O/σ-CH coupling. Furthermore, analogous to the C•/CH coupling from C(T)PR2 and (T)PR2 with 2-C(T)P in Figure 4, the C•/CH coupling can occur much easier than the C•/CCl coupling from the C(T)PDR and (T)PDR with 2-C(T)P in Figure 5. For example, in Figure 5(b), the C•/CH coupling from CTPDR + 2-CTP coupling (Δ*E* 2.27 kcal/mol, Δ*H* –24.80 kcal/mol) requires much lower potential barrier and is more exothermic than C•/CCl coupling (Δ*E* 11.78 kcal/mol, Δ*H* –9.30 kcal/mol). This implies the IM34 from C•/CH coupling is much easier to form than IM35 from C•/CCl coupling. To sum up, in Figure 5, the formation of IM30, IM32, IM34, IM36, IM38, IM40, IM42, IM44, IM46, IM48, IM50 and IM52 are much easier to form than IM31, IM32, IM35, IM37, IM39, IM41, IM43, IM45, IM47, IM49, IM51 and IM53, respectively. O(S)/σ-CH couplings can be followed by the elemination of H, ring closure and elemination of OH/SH to form PCDT/DFs, while the C•/CH coupling can be followed by the abstraction of H, ring closure and intramolecular elimination of SH/OH elimination to form PCDT/DFs

As illustrated in Figure 5, in terms of the enthalpically preferred C•/CH and O(S)/σ-CH couplings from C(T)PDR and (T)PDR with 2-C(T)P, the C•/CH coupling modes to form pre-PCDT/DF intermediates are more comparable the O(S)/σ-CH couplings modes to form pre-PCDT/DF intermediates. For instance, in Figure 5(a) and (d) the potential barriers involved in C•/CH modes to form keto-thioenol intermediates (0.61~1.29 kcal/mol) are generally lower than those involved in the correspongding O/σ-CH coupling modes (19.0~19.95 kcal/mol) to form ether-thioenol type intermediates. In addition, the C•/CH coupling modes are strongly exothermic by –27.41~–27.36 kcal/mol, while the O/σ-CH coupling are endothermic amounting to 9.71~10.30 kcal/mol in Figure 5(a) and (d). This is consistent with the values of CPDR + 2-CP and PDR + 2-CP couplings in Figure S1(c) and (e) of Supplementary Materials and totally contrary to the conclusion of CPR1 with 2-C(T)P in Figure 3 and Figure S1(a) that the O/C coupling are favored over the C/C coupling. To sum up, the most feasible pathway in each condensation in Figure 5(a)~(f) is the C•/CH coupling to form pre-PCDT/DF intermediates. In other words, IM30, IM34, IM38, IM42, IM46 and IM50 are the main intermediates from reactions of C(T)PDR and (T)PDR with 2-C(T)P. Obviously, according to Figure 5 and Figure S1(c) and (e), the formation potential ranking of most feasible routes from C(T)PDR with

2-C(T)P coupling is CPDR + 2-CTP > CPDR + 2-CP > CTPDR + 2-CTP > CTPDR + 2-CP; the formation potential ranking of of most feasible routes from(T)PDR with 2-C(T)P couplings is PDR + 2-CTP > PDR + 2-CP > TPDR + 2-CTP > TPDR + 2-CP.

In Figure 5, a much lower potential barrier is involved in the S/C couplings than that required in the O/C condensations by about 10 kcal/mol indicating that the S/C coupling pathways are more comparable than the O/C pathways. This agrees well with the conclusion above that the S/C coupling modes are overwhelmingly superior to the the O/C coupling modes. In contrary, the oxygen or sulfur substitution have little effect on the C•/CH or C•/CCl coupling, as the potential barriers and reaction heats of these coupling are similar, which is consistent with the coupling reactions of C(T)PR2 and (T)PR2 with 2-C(T)P.

3.2.4. Comparing the reactions of (thio)phenoxy radicals with 2-C(T)P couplings, sulfydryl/hydroxyl-substituted phenyl radicals with 2-C(T)P couplings and (thio)phenoxyl diradicals with 2-C(T)P couplings

To sum up, the thiophenoxy radicals with 2-C(T)P couplings in Figure 3 mainly produce the pre-PCTA/PT intermediates, with the potential barriers involved falling within 0.43 to 4.52 kcal/mol and reaction heats ranging from –0.48 to 10.65 kcal/mol. The sulfydryl/hydroxyl-substituted phenyl radicals with 2-C(T)P couplings in Figure 4 and the (thio)phenoxyl diradicals with 2-C(T)P couplings in Figure 5 can only generate PCDT/DF products. The potential barriers of the energetically favorable C•/CH coupling in Figure 4 are ranged from 1.93~4.14 kcal/mol, accompanied by reaction heats varying from –27.63~–24.94 kcal/mol. The potential barriers of the energetically more comparable C•/CH coupling in Figure 5 are amounted from 0.61~2.84 kcal/mol, and are simultaneously associated with strong exothermicities in the range of –27.41~–24.16 kcal/mol. Thus, the radical/molecule coupling of the three kinds radicals with 2-C(T)P demands virtually the same potential barriers. However, the pre-PCDT/DF intermediates formation from the sulfydryl/hydroxyl-substituted phenyl radicals with 2-C(T)P couplings and (thio)phenoxyl diradicals with 2-C(T)P couplings are much more exothermic than the pre-PCTA/PT intermediates formation from thiophenoxy radicals with 2-C(T)P couplings. It is evident that the pre-PCDT/DF intermediates are more easier to form and more stable than the pre-PCTA/PT intermediates. Thus, the PCDT/DFs are much more liable to form than PCTA/PTs from the radical/molecule coupling from 2-C(T)P as precursors. In particular, for the formation of PCTA/DTs from the three radical/molecule couplings from 2-CTP, the pre-PCDT intermediates formation pathways (ΔE 2.27~4.14 kcal/mol, ΔH –25.88~–24.80 kcal/mol) in Figure 4(b) and (e) and Figure 5(b) and (e) are overwhelmingly superior to the the pre-PCTA intermediates formation pathways (ΔE 0.43~4.28 kcal/mol, ΔH –0.48~10.65 kcal/mol) in Figure 3(b). This provides reasonable explanation for the high PCDT-to-PCTA ratio under the pyrolysis or combustion conditions [16,17].

3.3. Rate constant calculations

The thermodynamic analysis of formation from reactions of C(T)PR1 with 2-C(T)P and C(T)PDR and (T)PDR with 2-C(T)P shows that S/C coupling are preferred over O/C coupling. Comparing of the average calculated TST rate constants in these two couplings also approved this conclusion. For example, in Table 3, at 1000 K, the average TST rate constant for S/C coupling from reactions of C(T)PR1 with 2-C(T)P is 2.60×10^{-16} cm^3 molecule^{-1} s^{-1}, which is larger than the value 1.75×10^{-20} cm^3 molecule^{-1} s^{-1} for O/C coupling from reactions of C(T)PR1 with 2-C(T)P. Analogously, the average TST rate constant for S/C coupling from reactions of C(T)PDR and (T)PDR with 2-C(T)P (1.59×10^{-17} cm^3 molecule^{-1} s^{-1}) is kinetically larger than that of O/C coupling from reactions of C(T)PDR and (T)PDR with 2-C(T)P (3.24×10^{-20} cm^3 molecule^{-1} s^{-1}).

As presented in Table 1, Table 2 and Table S2 of Supplementary Materials, the TST rate constants for C•/CH coupling are larger than those of C•/CCl coupling from coupling reactions of C(T)PR2 and (T)PR2 with 2-C(T)P and coupling reactions of C(T)PDR and (T)PDR with 2-C(T)P over the whole studied temperature range. For instance, at 1000 K, the TST rate constants for the formation of IM19, IM21, IM23, IM25, IM27 and IM29 from C•/CH coupling are 6.32×10^{-16}, 1.33×10^{-16}, 5.54×10^{-16}, 3.11

Peer-reviewed version available at Int. J. Mol. Sci. 2019, 20, 1542; doi:10.3390/ijms20071542

× 10^{-16}, 1.84 × 10^{-16} and 9.70 × 10^{-16}, while the values are 7.01 × 10^{-18}, 6.31 × 10^{-19}, 7.82 × 10^{-18}, 3.72 × 10^{-18}, 3.95 × 10^{-19} and 1.02 × 10^{-17} for the formation of IM20, IM22, IM24, IM26, IM28, IM26 from C•/CCl coupling in Table 1 and Table S2 of Supplementary Materials. In addition, at 800 K, the TST rate constants for the C•/CH coupling reaction of CTPDR + 2-CTP → IM34 via TS63 (1.73 × 10^{-16} cm^3 molecule^{-1} s^{-1}) is larger than that of for the C•/CCl reaction of CTPDR + 2-CTP → IM35 via TS64 (1.15 × 10^{-19} cm^3 molecule^{-1} s^{-1}) in Table 2 and Table S2 of Supplementary Materials. This perfectly matches the thermodynamic analysis above that C•/CH coupling are kinetically more efficient than the C•/CCl coupling.

Similarly, the kinetic data also can confirm the thermodynamic analysis from reactions of C(T)PR1 with 2-C(T)P and C(T)PDR and (T)PDR with 2-C(T)P that the S/σ-CH coupling is more readily to occur than the S/σ-CCl coupling over the whole studied temperature range. For instance, at 800 K, the TST rate constants for the S/σ-CH coupling reaction of CTPR1 + 2-CTP → IM7 via TS35 is 1.34 × 10^{-16} cm^3 molecule^{-1} s^{-1}, which is larger than the calculated value for the S/σ-CCl reaction of CTPR1 + 2-CTP → IM8 via TS36 is 7.14 × 10^{-18} cm^3 molecule^{-1} s^{-1} in Table 1 and Table S2 of Supplementary Materials. In addition, at 1000 K, the TST rate constants for the S/σ-CH coupling reaction of CTPDR + 2-CTP → IM36 via TS65 (1.49 × 10^{-17} cm^3 molecule^{-1} s^{-1}) is larger than that of for the S/σ-CCl reaction of CTPDR + 2-CTP → IM37 via TS66 (4.20 × 10^{-19} cm^3 molecule^{-1} s^{-1}) in Table 2 and Table S2 of Supplementary Materials.

4. Materials and Methods

4.1. Density Functional Theory

All the quantum chemical calculations on the structure, frequency and energy of related substances such as reactants, products, intermediates, transition state were performed by using the Gaussian 09 program by using MPWB1K method [51]. The MPWB1K method is one of the best efficient and high-precision configuration optimization and frequency calculation method relative to computational cost [52], and has been successfully performed for formation of PCDT/TAs from 2,4-DCTP as precursor [26]. Geometries were optimized at the MPWB1K/6-31+G(d,p) level of theory. The obtained structures were confirmed as stable configuration or transition state by using corresponding frequency calculation at the same level. The intrinsic reaction coordinate (IRC) was calculated at the MPWB1K/6-31+G(d,p) level to verify that the transition state connects to the right minima along the reaction path [53]. In order to get more precise energy values, a more flexible basis set, 6-311+G(3df,2p), was employed to determine the single point energies, including zero-point energy correction (ZPE).

4.2. Kinetic Calculation

The kinetic and statistical thermodynamic (KiSThelP) program, a cross-platform free open-source program developed to estimate molecule and reaction properties from electronic structure data, was used to calculate the reaction rate constants [49]. KiSThelP offers a range of features that can be helpful for users more experienced in computational kinetics. The conventional transition state theory (TST) method was applied to calculate the rate constants for all the radical/molecule combination reactions in the typical temperature of incinerator (from 600~1200 K). The effect of quantum tunneling on rate constants was considered based on the one-dimensional Wigner's formalism as implemented in the KiSThelP program [50].

5. Conclusion

In the study the radical/molecule initial formation pathways of PCTA/PT/DT/DFs from the cross-condensation reactions of chloro(thio)phenoxy radical, sulfydryl/hydryl-substituted phenyl radical and (thio)phenoxyl diradical with 2-C(T)P were investigated theoretically using DFT electronic structure theory at the MPWB1K/6-31+G(d,p)//MPWB1K/6-31+G(d,p) level. The kinetic calculation was performed and the rate constants were calculated over the temperature range of 600~1200 K using the conventional transition state theory (TST) method, which can afford accurate input parameters for the dioxin formation models. The values were compared with the previous studies on the radical/radical formation mechanism of PCTA/DFs from CTPRs and the radical/molecule formation mechanism of PCDFs from oxygen substituted radicals with CP [26]. Our study found that the radical/molecule mechanism can contribute to the gas-phase formation of PCTA/PT/DT/DFs under the pyrolysis or combustion conditions, which has been ignored before. previous work [26] indicated that the radical/molecule coupling of chlorophenoxy radical, hydryl-substituted phenyl radical and phenoxyl diradical with 2-CP can only form pre-PCDFs intermediates, and the O/C coupling to form pre-PCDDs intermediates failed to occur. However, we found in this study that the radical/molecule coupling of sulfur sustituted chlorothiophenoxy radical, sulfydryl-substituted phenyl radical and thiophenoxyl diradical with 2-CTP could contribute to both the formation of pre-PCDTs and pre-PCTAs intermediates. Four conclusions can be summarized as follows:

(1) The S/C coupling modes are preferable over the O/C coupling modes. The S/C coupling modes can form pre-PCTAs and pre-PCPTs intermediates in in the coupling of chloro(thio)phenoxy radical with 2-C(T)P and form pre-PCDTs intermediates in the coupling of (thio)phenoxyl diradical with 2-C(T)P.

(2) For the self-coupling of 2-CTP and corresponding sulfur substituted radicals, the pre-PCTA intermediates can only be produced from the coupling of chlorothiophenoxy radical with 2-CTP, and the pre-PCTA intermediates can be formed both the coupling of sulfydryl-substituted phenyl radicaland with 2-CTP and the coupling of thiophenoxyl diradical with 2-CTP. The pre-PCDT intermediates formation pathways are more favorable to the the pre-PCTA intermediates formation pathways, which, to some extent, can give reasonable explanation for the high PCDT-to-PCTA ratio under the pyrolysis or combustion conditions.

(3) The S(O)/σ-CH couplings are energetically more comparable than the S(O)/σ-CCl couplings, and the C•/CH coupling can take place much easier than the C•/CCl coupling to form the (thio)keto-(thio)enol intermediates.

(4) In the coupling of chloro(thio)phenoxy radical with 2-C(T)P, the S/C coupling to form pre-PCTA/PTs intermediates are more readily to occur than the C/C coupling to form pre-PCDT/DFs intermediates. However the turn is contrast in the coupling of (thio)phenoxyl diradical with 2-C(T)P that C/C coupling are more easier to happen than the S/C coupling, both of which can contribute to the formaiton of pre-PCDT/DFs intermediates.

Supplementary Materials: Pre-PCDD/DF formation pathways embedded with the potential barriers Δ*E* and reaction heats Δ*H* from the coupling reactions of CPR1 with 2-CP, CPR2 with 2-CP and CPDR with 2-CP, PR2 with 2-CP and PDR with 2-CP. The optimized geometries for transition states for pre-PCTA formation routes from the S/C coupling of cross-condensation reactions of CTPR1 with 2-CTP. Optimized geometries for transition states of the coupling reactions of CTPR1 with 2-CTP, CTPR2 with 2-CTP, CTPDR with 2-CTP, CPR1 with 2-CP and PR2 with 2-CP. Imaginary frequencies, zero point energies and total energies for transition states involved in the formation of pre-PCTA/PT/DT/DF intermediates. TST rate constants for for pre-PCTA/PT/DT/DF formation routes from the cross-condensation reactions of 2-C(T)P with C(T)PR1, C(T)PR2 and (T)PR2, and C(T)PDR and (T)PDR over the temperature range of 600~1200 K. Cartesian coordinates for transition states, reactions, intermediate and products involved in the formation routes of pre-intermediates for PCTA/PT/DT/DFs. Supplementary materials can be found at www.mdpi.com/xxx/s1.

Author Contributions: Chenpeng Zuo designed and performed the mechanism calculations, then wrote the manuscript; Chenpeng Zuo, Hetong Wang and Siyuan Zheng performed the kinetic calculation. Chenpeng Zuo, Wenxiao Pan, Fei Xu and Qingzhu Zhang all analyzed the data in the manuscript.

Funding: This work was supported by NSFC (National Natural Science Foundation of China, project Nos. 21677089), Shenzhen Science and Technology Research and Development Funds (project Nos. JCYJ20160510165106371), FRFSDU(The Fundamental Research Funds of Shandong University, project Nos. 2016WLJH51, 2017JC033), China Postdoctoral Science Foundation funded project (project Nos. 2017M612277, 2017T100493), SKLECRA (The open foundation of state key laboratory of environmental criteria and risk assessment, Chinese research academy of environmental sciences No. 2016OFP09).

Conflicts of Interest: The authors declare no conflict of interest.

Abbreviations

PCDTs	polychlorinated dibenzothiophenes
PCPTs	polychlorinated phenoxathiins
PCTAs	polychlorinated thianthrenes
PCDDs	polychlorinated dibenzo-p-dioxins
PCDFs	polychlorinated dibenzofurans
2-CP	2-chlorophenol
2-CTP	2-chlorothiophenol
CPR1	2-chlorophenoxy
CPR2	2-hydroxyl-3-chloro-phenyl
CPDR	chlorinated phenoxyl diradical
PR2	2-hydroxylphenyl radical
PDR	phenoxyl diradical
CTPR1	2-chlorothiophenoxy
CTPR2	2-sulfydryl-3-chloro-phenyl
CTPDR	chlorinated thiophenoxyl diradical
TPR2	2-sulfydrylphenyl radical
TPDR	thiophenoxyl diradical
TST	transition state theory
IRC	intrinsic reaction coordinate
KiSThelP	kinetic and statistical thermodynamic
ZPE	zero-point energy

References

1. Wang, Y.; Zeng, X.L.; Chen, H.J.; Wang, H.J. Thermodynamic properties and relative stability of polychlorinated thianthrenes by density functional theory. *J. Chem. Eng. Data* **2007**, *52*, 1442−1448.
2. Chen, S.D.; Liu, H.X.; Wang, Z.Y. Study of structural and thermodynamic properties for polychlorinated dibenzothiophenes by density functional theory. *J. Chem. Eng. Data* **2007**, *52*, 1195−1202.
3. Sinkkonen, S. New types of persistent halogenated compounds. *Springer* **2000**, *3*, 289−314.
4. Puzyn, T.; Rostkowski, P.; Swieczkowski, A.; Jędrusiak, A.; Falandysz, J. Prediction of environmental partition coefficients and the Henry's law constants for 135 congeners of chlorodibenzothiophene. *Chemosphere* **2006**, *62*, 1817−1828.
5. Kopponen, P.; Sinkkonen, S.; Poso, A.; Gynther, J.; Karenlampi, S. Sulfur analogues of polychlorinated dibenzo-p-dioxins, dibenzofurans and diphenyl ethers as inducers of CYP1A1 in mouse hepatoma cell culture and structure-activity relationships. *Environ. Toxicol. Chem.* **1994**, *13*, 1543−1548.
6. Weber, R.; Hagenmaier, H.; Schrenk, D. Elimination kinetics and toxicity of 2,3,7,8-tetrachlorothiantheren, a thio analogue of 2,3,7,8-TCDD. *Chemosphere* **1998**, *36*, 2635−2641.
7. Nakai, S.; Espino, M.P.; Nomura, Y.; Hosomi, M. Detection of polychlorinated dibenzothiophenes (PCDTs) in the environmental samples and investigation of their photodegradability and dioxin-like endocrine disruption potentcy. *J. Environ. Chem.* **2004**, *14*, 835−844.
8. Buser, H.R.; Rappe, C. Determination of polychlorodibenzothiophenes, the sulfur analogs of polychlorodibenzofurans, using various gas chromatographic/mass spectrometric techniques. *Anal. Chem.* **1991**, *63*, 1210−1217.
9. Sinkkonen, S.; Paasivirta, J.; Lahtipera, M. Chlorinated and methylated dibenzothiophenes in sediment samples from a river contaminated by organochlorine wastes. *J. Soils Sediments* **2001**, *1*, 9−14.
10. Pruell, R.J.; Rubinstein, N.I.; Taplin, B.K.; Livolsi, J.A.; Bowen, R.D. Accumulation of polychlorinated organic contaminants from sediment by three benthic marine species. *Arch. Environ. Contam. Toxicol.* **1993**, *24*, 290−297.
11. Sinkkonen, S.; Kolehmainen, E.; Paasivirta, J.; Koistinen, J.; Lahtipera, M.; Lammi, R. Identification and level estimation of chlorinated neutral aromatic sulfur compounds and their alkylated derivatives in pulp mill effluents and sediments. *Chemosphere* **1994**, *28*, 2049−2066.
12. Sato, S.; Matsumura, A.; Urushigawa, Y.; Metwally, M.; Al-Muzaini, S. Structural analysis of weathered oil from Kuwait's environment. *Environ. Int.* **1998**, *24*, 77−87.

13. Atlas, R.M. Fate of oil from two major oil spills: Role of microbial degradation in removing oil from the Amoco Cadiz and IXTOC I spills. *Environ. Int.* **1981**, *5*, 33–38.
14. Buser, H.R. Identification and sources of dioxin-like compounds: I. polychlorodibenzothiophenes and polychlorothianthrenes, the sulfur-analogues of the polychlorodibenzofurans and polychlorodibenzodioxins. *Chemosphere* **1992**, *25*, 45–48.
15. Sinkkonen, S.; Paasivirta, J.; Koistinen, J.; Tarhanen, J. Tetra- and pentachlorodibenzothiophenes are formed in waste combustion. *Chemosphere* **1991**, *23*, 583–587.
16. Sinkkonen, S.; Kolehmainen, E.; Koistinen, J.; Lahtipera, M. High-resolution gas chromatographic-mass spectrometric determination of neutral chlorinated aromatic sulphur compounds in stack gas samples. *J. Chromatogr. A* **1993**, *641*, 309–317.
17. Sinkkonen, S.; Vattulainen, A.; Aittola, J.P.; Paasivirta, J.; Tarhanen, J.; Lahtipera, M. Metal reclamation produces sulphur analogues of toxic dioxins and furans. *Chemosphere* **1994**, *28*, 1279–1288.
18. Sinkkonen, S.; Paasivirta, J.; Koistinen, J.; Lahtipera, M.; Lammi, R. Polychlorinated dibenzothlophenes in bleached pulp mill effluents. *Chemosphere* **1992**, *24*, 1755–1763.
19. Mostrąg, A.; Puzyn, T.; Haranczyk, M. Modeling the overall persistence and environmental mobility of sulfur-containing polychlorinated organic compounds. *Environ. Sci. Pollut. Res.* **2010**, *17*, 470-477.
20. Wiedmann, T.; Riehle, U.; Kurz, J.; Ballschmiter, K. HRGC-MS of polychlorinated phenanthrenes (PCPhen), dibenzothiophenes (PCDT), dibenzothianthrenes (PCTA), and phenoxathiins (PCPT). *Fresenius J. Anal. Chem.* **1997**, *359*, 176-188.
21. Ferrario, E. Preparation of phenoxathiin from diphenyl ether and sulfur. *Bull. Soc. Chim.* **1911**, *9*, 536-537.
22. Bourke, J.B., Felsot, A.S., Gilding, T.J., Jensen, J.K. Seiber, J.N. *Pesticide waste management*, ACS Symposium Series, American Chemical Society: Washington, DC, USA, 1992; pp. 157–165.
23. Dar, T.; Altarawneh, M.; Dlugogorski, B. Theoretical study in the dimerisation of 2-chlrothiophenol/2-chlorothiophenoxy: precursors to PCDT/TA. *Organohalogen Compd.* **2012**, *74*, 657–660.
24. Dar, T.; Altarawneh, M.; Dlugogorski, B.Z. Quantum chemical study on formation of PCDT/TA from 2-chlorothiophenol precursor. *Environ. Sci. Technol.* **2013**, *47*, 11040–11047.
25. Dar, T.; Shah, K.; Moghtaderi, B.; Page, A.J. Formation of persistent organic pollutants from 2,4,5-trichlorothiophenol combustion: a density functional theory investigation. *J. Mol. Model.* **2016**, *22*, 128.
26. Xu, F.; Shi, X.L.; Li, Y.F.; Zhang, Q.Z. Mechanistic and kinetic studies on the homogeneous gas-phase formation of PCTA/DTs from 2,4-dichlorothiophenol and 2,4,6-trichlorothiophenol. *Int. J. Mol. Sci.* **2015**, *16*, 20449–20467.
27. Yu, X.Q.; Chang, J.M.; Liu, X.; Pan, W.X.; Zhang, A.Q. Theoretical study on the formation mechanism of polychlorinated dibenzothiophenes/thianthrenes from 2-chlorothiophenol molecules. *J. Environ. Sci.* **2018**, *66*, 318–327.
28. Parette, R.; Pearson, W.N. 2,4,6,8-Tetrachlorodibenzothiophene in the Newark Bay Estuary: The likely source and reaction pathways. *Chemosphere* **2014**, *111*, 157–163.
29. Navarro, R.; Bierbrauer, K.; Mijangos, C.; Goiti, E.; Reinecke, H. Modification of poly (vinyl chloride) with new aromatic thiol compounds. Synthesis and characterization. *Polym. Degrad. Stab.* **2008**, *93*, 585–591.
30. Buisson, R.; Kirk, P.; Lester, J. Determination of chlorinated phenols in water, wastewater, and wastewater sludge by capillary GC/ECD. *J. Chromatogr. Sci.* **1984**, *22*, 339–342.
31. Wegman, R.C.C.; Van den Broek, H.H. Chlorophenols in river sediment in the Netherlands. *Water Res.* **1983**, *17*, 227–230.
32. Briois, C.; Visez, N.; Baillet, C.; Sawerysyn, J.P. Experimental study on the thermal oxidation of 2-chlorophenol in air over the temperature range 450–900 °C. *Chemosphere* **2006**, *62*, 1806–1816.
33. Kaiser, R.; Parker, D.; Zhang, F.; Landera, A.; Kislov, V.; Mebel, A. PAH formation under single collision conditions: reaction of phenyl radical and 1,3-butadiene to form 1,4-dihydronaphthalene. *J. Phys. Chem. A* **2012**, *116*, 4248–4258.
34. Shukla, B.; Susa, A.; Miyoshi, A.; Koshi, M. Role of phenyl radicals in the growth of polycyclic aromatic hydrocarbons. *J. Phys. Chem. A* **2008**, *112*, 2362–2369.
35. Bonnichon, F.; Richard, C.; Grabner, G. Formation of an α-ketocarbene by photolysis of aqueous 2-bromophenol. *Chem. Commun.* **2001**, 73–74.
36. Pan, W.X.; Zhang, D.J.; Han, Z.; Zhan, J.H.; Liu, C.B. New insight into the formation mechanism of PCDD/Fs from 2-chlorophenol precursor. *Environ. Sci. Technol.* **2013**, 47, 8489-8498.

Preprints (www.preprints.org) | NOT PEER-REVIEWED | Posted: 26 February 2019 doi:10.20944/preprints201902.0237.v1

Peer-reviewed version available at *Int. J. Mol. Sci.* **2019**, *20*, 1542; doi:10.3390/ijms20071542

37. Evans, C.S.; Dellinger, B. Mechanisms of dioxin formation from the high-temperature pyrolysis of 2-chlorophenol. *Environ. Sci. Technol.* **2003**, *37*, 1325–1330.
38. Evans, C.S.; Dellinger, B. Mechanisms of dioxin formation from the high-temperature oxidation of 2-chlorophenol. *Environ. Sci. Technol.* **2005**, *39*, 122–127.
39. Zhang, Q.Z.; Li, S.Q.; Qu, X.H.; Shi, X.Y.; Wang, W.X. A quantum mechanical study on the formation of PCDD/Fs from 2-chlorophenol as precursor. *Environ. Sci. Technol.* **2008**, *42*, 7301–7308.
40. Qu, X.H.; Wang, H.; Zhang, Q.Z.; Shi, X.Y.; Xu, F.; Wang, W.X. Mechanistic and kinetic studies on the homogeneous gas-phase formation of PCDD/Fs from 2,4,5-trichlorophenol. *Environ. Sci. Technol.* **2009**, *43*, 4068–4075.
41. Pan, W.X.; Fu, J.J.; Zhang, A.Q. Theoretical study on the formation mechanism of pre-intermediates for PXDD/Fs from 2-Bromophenol and 2-Chlorophenol precursors via radical/molecule reactions. *Environ. Pollut.* **2017**, *225*, 439–449.
42. Sinkkonen, S. Sources and environmental fate of PCDTs. *Toxicol Environ. Chem.* **1998**, 66, 105–112.
43. Czerwinski, J. Pathways of polychlorinated dibenzothiophenes (PCDTs) in the environment. *Arch. Environ. Prot.* **2008**, *34*, 169–181.
44. Zhang, Q.Z.; Qu, X.H.; Wang, H.; Xu, F.; Shi, X.Y.; Wang, W.X. Mechanism and thermal rate constants for the complete series reactions of chlorophenols with H. *Environ. Sci. Technol.* **2009**, *43*, 4105–4112.
45. Xu, F.; Wang, H.; Zhang, Q.Z.; Zhang, R.X.; Qu, X.H.; Wang, W.X. Kinetic properties for the complete series reactions of chlorophenols with OH radicals–relevance for dioxin formation. *Environ. Sci. Technol.* **2010**, *44*, 1399–1404.
46. Xu, F.; Shi, X.L.; Zhang, Q.Z.; Wang, W.X. Formation of chlorotriophenoxy radicals from complete series reactions of chlorotriophenols with H and OH radicals. *Int. J. Mol. Sci.* **2015**, *16*, 18714–18731.
47. Parker, D.S.N.; Kaiser, R.I.; Troy, T.P.; Kostko, O.; Ahmed, M.; Mebel, A.M. Toward the oxidation of the phenyl radical and prevention of PAH formation in combustion systems. *J. Phys. Chem. A* **2014**, *119*, 7145–7154.
48. Kislov, V.V.; Mebel, A.M. Ab initio/RRKM-ME study on the mechanism and kinetics of the reaction of phenyl radical with 1,2-butadiene. *J. Phys. Chem. A* **2010**, *114*, 7682–7692.
49. Canneaux, S.; Bohr, F.; Henon, E. KiSThelP: A program to predict thermodynamic properties and rate constants from quantum chemistry results. *J. Comput. Chem.* **2014**, *35*, 82–93.
50. Wigner, E. Calculation of the rate of elementary association reactions. *J. Chem. Phys.* **1937**, *5*, 720–725.
51. Frisch, M.J.; Trucks, G.W.; Schlegel, H.B.; Scuseria, G.E.; Robb, M.A.; Cheeseman, J.R.; Scalmani, G.; Barone, V.; Mennucci, B.; Petersson, G.A.; *et al. Gaussian 09, revision A.02*; Gaussian, Inc.: Wallingford, CT, USA, 2009.
52. Zhao, Y.; Truhlar, D.G. Hybrid meta density functional theory methods for therochemistry, thermochemical kinetics, and noncovalent interactions: the MPW1B95 and MPWB1K models and comparative assessments for hydrogen bonding and van der Waals interactions. *J. Phys. Chem. A* **2004**, *108*, 6908–6918.
53. Fukui, K. The path of chemical reactions—The IRC approach. *Acc. Chem. Res.* **1981**, *14*, 363–368.